

# COPPER AND ITS ALLOYS

UDC 669.3.017:691.735:620.17-18

## MICROSTRUCTURE AND PROPERTIES OF Cu – Cr – Zr ALLOYS AFTER PLASTIC DEFORMATION AND AGING

A. I. Bodyakova,<sup>1</sup> R. V. Mishnev,<sup>1</sup> and R. O. Kaibyshev<sup>1,2</sup>Translated from *Metallovedenie i Termicheskaya Obrabotka Metallov*, No. 6, pp. 24 – 36, June, 2024.*Original article submitted November 29, 2023.*

The microstructure of alloys of the Cu – Cr – Zr system after equal channel angular pressing and aging is investigated by scanning and transmission electron microscopy. Mechanical properties and electrical conductivity are determined. Recovery and additional precipitation of dispersed particles are observed in deformed alloys after annealing at temperatures of 200 – 500°C, but static recrystallization does not develop. Increasing the annealing temperature to 600°C is accompanied by development of recrystallization, and a completely recrystallized structure is observed within the alloy with a minimum content of alloying elements, while deformed areas are found in alloys with a high content of chromium and zirconium. The influence of structural evolution on mechanical properties and electrical conductivity is discussed.

**Key words:** Cu – Cr – Zr alloys, plastic deformation, aging, microstructure, mechanical properties, hardness, electrical conductivity.

### INTRODUCTION

Low-alloy copper alloys of the Cu – Cr – Zr system are thermally strengthened alloys, which due to good strength properties and electrical conductivity find application within many branches of the electrical engineering industry with preparation of conductor contacts, contact welding electrodes, electric motor commutators, contact conductors for high-speed railways, etc. [1 – 4]. Performance of heat treatment for a supersaturated solid solution with subsequent ageing facilitates formation within the structure of fine Cr and Cu<sub>3</sub>Zr particles, which provide an increase in alloy strength properties by 100 – 150 MPa [5 – 9]. In this case separation of particles causes a reduction in the concentration of substitution atoms within a copper matrix, which facilitates preparation of good electrical conductivity properties (more than 80% of the electrical conductivity of pure copper) (% IACS) [10, 11].

An additional increase in strength without a significant reduction in electrical conductivity may be added due to use of plastic deformation methods [11, 12], such as equal channel angular pressing (ECAP). It has been demonstrated that ECAP according to the Conform system may be used for producing long workpieces and subsequent adaptation for industrial production [13, 14]. Performance of ECAP for low-alloy copper Cu – Cr – Zr alloys facilitates formation of a high density of low-angle boundaries of deformation origin which increases their misorientation with an increase in the degree of deformation and they are transformed into large-angle boundaries. Therefore, during ECAP there is original grain refinement and formation of an ultrafine grain (UFG) structure with a high dislocation density [15 – 17]. These structures exhibit high internal stresses and are characterized by a high moving force for development of static recrystallization. For a pure copper UFG the temperature for the start of relaxation is 160°C, which about 60°C below for coarse-grained copper [18]. It is well known [5, 19 – 28] that the annealing temperature with which hardness of Cu – Cr – Zr-alloys is reduced by 20% is within the temperature range 500 – 600°C (Fig. 1). However, the effect of alloy-

<sup>1</sup> Belgorod State National Research University, Belgorod, Russia (e-mail: bodyakova-ai@yandex.ru).

<sup>2</sup> Russian State Agrarian University, K. A. Timiryazev Agricultural Academy, Moscow, Russia.

**TABLE 1.** Chemical Composition of Alloys of the Cu – Cr – Zr System Studied

Alloy	Element content,* wt. %	
	Cr	Zr
Cu – 0.1Cr – 0.1Zr	0.10	0.06
Cu – 0.3Cr – 0.5Zr	0.30	0.50
Cu – 0.8Cr – 0.1Zr	0.87	0.06

\* Balance copper.

ing elements within these alloys on development of static recovery and recrystallization, as for the main softening factor, has not been studied adequately within publications.

The aim of the present work is a study of the effect of chemical composition on recovery and recrystallization processes, and also the change in mechanical properties and electrical conductivity of low alloy Cu – Cr – Zr-alloys after ECAP and annealing at different temperatures.

## METHODS OF STUDY

Three Cu – Cr – Zr-alloys were studied with different Cr and Zr contents, whose chemical composition is provided in Table 1. Alloys were prepared using casting into a mold. Workpieces were subjected to heating by a regime: exposure within a muffle furnace at 920°C for 1 h, water cooling in order to obtain a supersaturated solid solution, and aging for maximum strength. The effect of aging temperature and time on strength and electrical conductivity of the alloys in question is similar to that discussed in [6]. Alloys Cu – 0.9Cr – 0.1Zr and Cu – 0.3Cr – 0.5Zr<sup>3</sup> were subjected to aging at 450°C, 1 h, and alloy Cu – 0.1Cr – 0.1Zr at 550°C, 4 h cooling after aging was accomplished in water. From billets specimens were cut with a size of 12 × 12 × 100 mm and ECAP was conducted within equipment with an intersection angle for die channels of 90° over a  $B_C$  path. The ECAP temperature for alloys Cu – 0.1Cr – 0.1Zr and Cu – 0.3Cr – 0.5Zr was 400°C, and for alloy Cu – 0.9Cr – 0.1Zr it was 200°C. There was accomplishment of 12, 8 and 4 ECAP passes for alloys Cu – 0.1Cr – 0.1 Zr, Cu – 0.9Cr – 0.1Zr and Cu – 0.3Cr – 0.5Zr respectively. Plastic deformation accomplished formation within alloys of an UFG structure with a similar grain size of the order to 1 μm. The alloys were annealed in the temperature range 200 – 700 for 1 h followed by water cooling.

Microstructural analysis was performed by means of a Quanta 600 Fei scanning electron microscope fitted with an attachment for analyzing back scattered electron diffraction. Specimens for study were subjected to treatment upon grinding paper with a different grain size and polished with diamond paste with an abrasive element size of the order to

<sup>3</sup> Here and subsequently throughout the test alloy composition (apart from indicated cases) is given in fractions, expressed as a %.

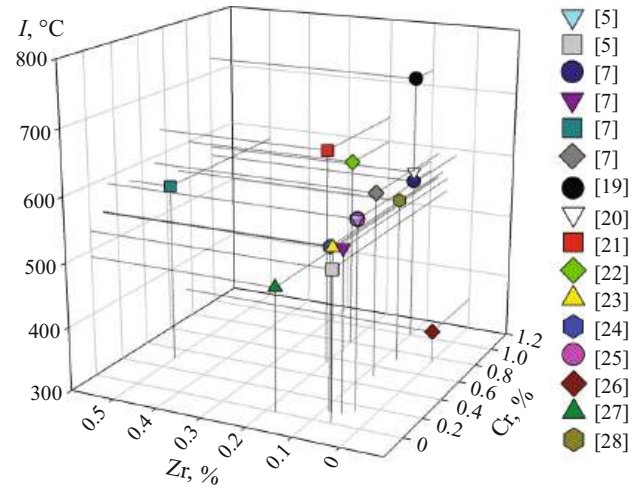


**Fig. 1.** Dependence of weakening temperature ( $T$ ) on chemical composition of alloys of the Cu – Cr – Zr system.

3 μm. Then electrochemical polishing was accomplished within 25% HNO<sub>3</sub> + 75% CH<sub>2</sub>OH at room temperature and a voltage of 10 V. Maps were plotted by means of OIM Analysis software for the crystallite boundary distribution, and for microdeformation (Kernel Average Misorientation function) and scatter of misorientation within a grain (Grain Orientation Spread function). The average grain size was determined by averaging horizontal and vertical sections, and the average boundary misorientation angle and proportion of large angle boundaries (LAB) (boundary between crystallites with a misorientation angle > 15°), microdeformation (average angle between two neighboring points of a study separated by the scanning pitch), average scatter and misorientation within a grain, dislocation density, calculated from misorientations and low angle boundaries (LAB) density, were determined by means of an approach proposed in [29]. Transmission electron microscopy (TEM) was performed within a JEOL 2100 microscope. Specimens were prepared by electrochemical polishing within a 25% HNO<sub>3</sub> – 75% CH<sub>3</sub>OH electrolyte at 20°C and a voltage of 10 V.

Mechanical properties were determined in uniaxial tension in an Instron 5882 equipment. The deformation rate was 2 mm/min. Vickers hardness was determined in a Wolpert 420 MVD test machine with a load upon the indenter of 200 g, exposure time 15 sec. Loss of strength  $F_{HV}$  was determined by an equation

$$F_{HV} = \frac{HV_{def} - HV_i}{HV_{def} - HV_{rec}}, \quad (1)$$

where  $HV_{def}$  is alloy hardness after deformation;  $HV_i$  is hardness after the corresponding treatment;  $HV_{rec}$  is alloy hardness within an entirely recrystallized condition.

Electrical conductivity was measured by a vortex method using a Konstanta K-6 measuring instrument. The proportion of supersaturated solid solution decomposition ( $F_{deco}$ ) was

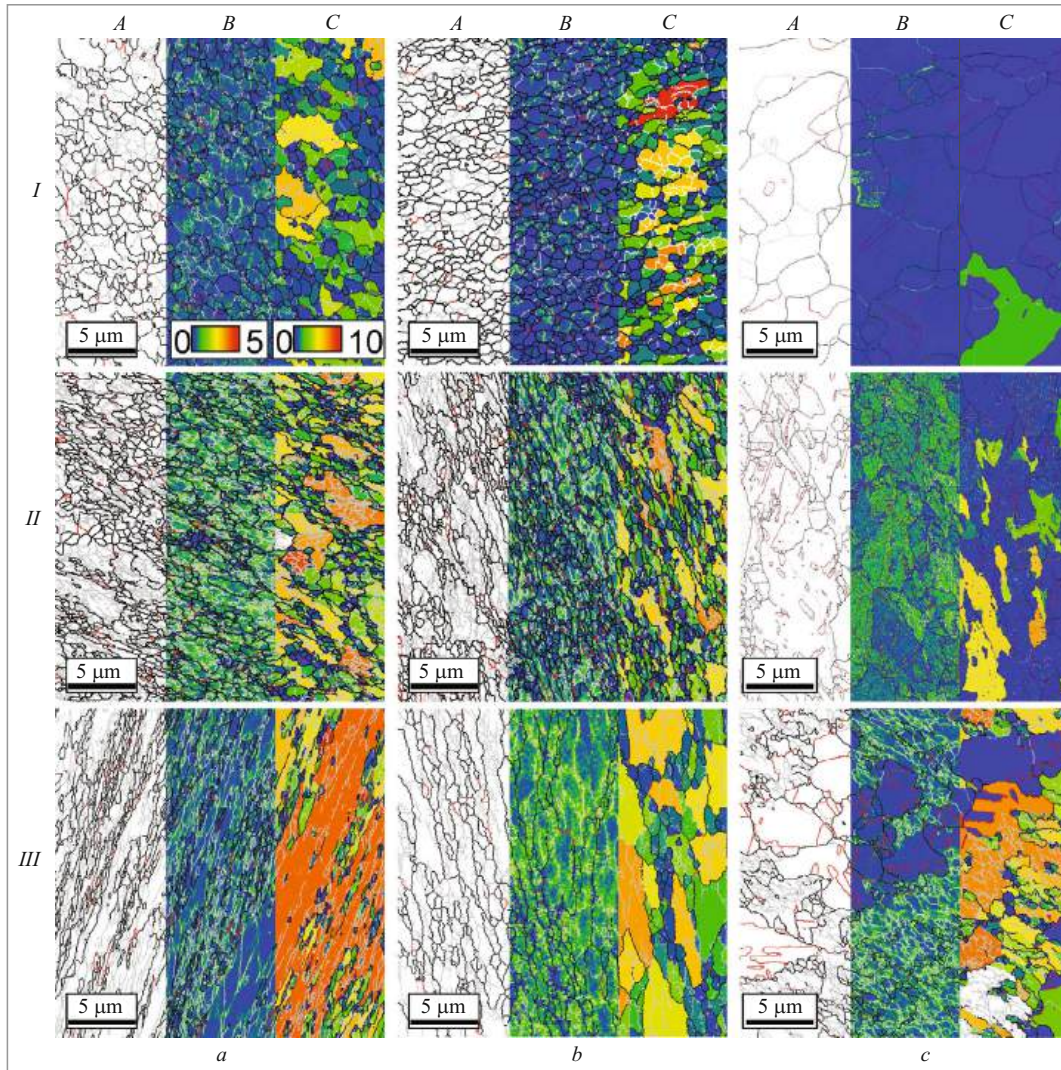


**Fig. 2.** Microstructure of alloys Cu – 0.1Cr – 0.1Zr (I), Cu – 0.9Cr – 0.1Zr (II) and Cu – 0.3Cr – 0.5Zr (III) after deformation (a), deformation and annealing at 500°C (b) and 600°C (c). Presented for each condition: A) grain boundary distribution map (black lines are LAB; gray lines are SAB; red lines are  $\Sigma 3$  boundaries; B) is micro-strain map; C) is scatter of orientations within a grain.

determined from the change in electrical conductivity in accordance with the procedure in [30].

## RESULTS AND DISCUSSION

**Microstructure.** Distribution maps are provided in Fig. 2 for typical microstructures formed within alloys after deformation and annealing at different temperatures. During deformation within Cu – Cr – Zr-alloys there is formation of SAB, which increase misorientation with an increase in the degree of deformation and they are transformed into LAB [10, 15 – 17, 31]. Therefore, after ECAP to the greatest extent there is formation of a UFG structure with a proportion of LAB of about 50%. The form of new ultrafine grains was similar to equilibrium. Within alloys Cu – 0.1Cr – 0.1Zr and Cu – 0.3Cr – 0.5Zr microdeformation is concentrated mainly

close to SAB, whereas within alloys Cu – 0.9Cr – 0.1Zr a high level of microdeformation is observed within grains. After deformation within all alloys considerable scatter is observed for misorientation within grains. Annealing in the temperature range 200 – 500°C does not lead to marked changes within the microstructure. It may be noted that the level of microdeformation and misorientation scatter within a grain is reduced a little, which may be a consequence of development of recovery. An increase in annealing temperature to 600°C is accompanied by development of static recrystallization. Grain size increases, the proportion of SAB decreases, and there is formation of a considerable twin boundaries  $\Sigma 3$ . The level of microdeformation and scatter of intergranular misorientations is reduced considerably. Within alloy Cu – 0.9Cr – 0.1Zr and entirely recrystallized structure is observed, but within alloys Cu – 0.9Cr – 0.1Zr and Cu –

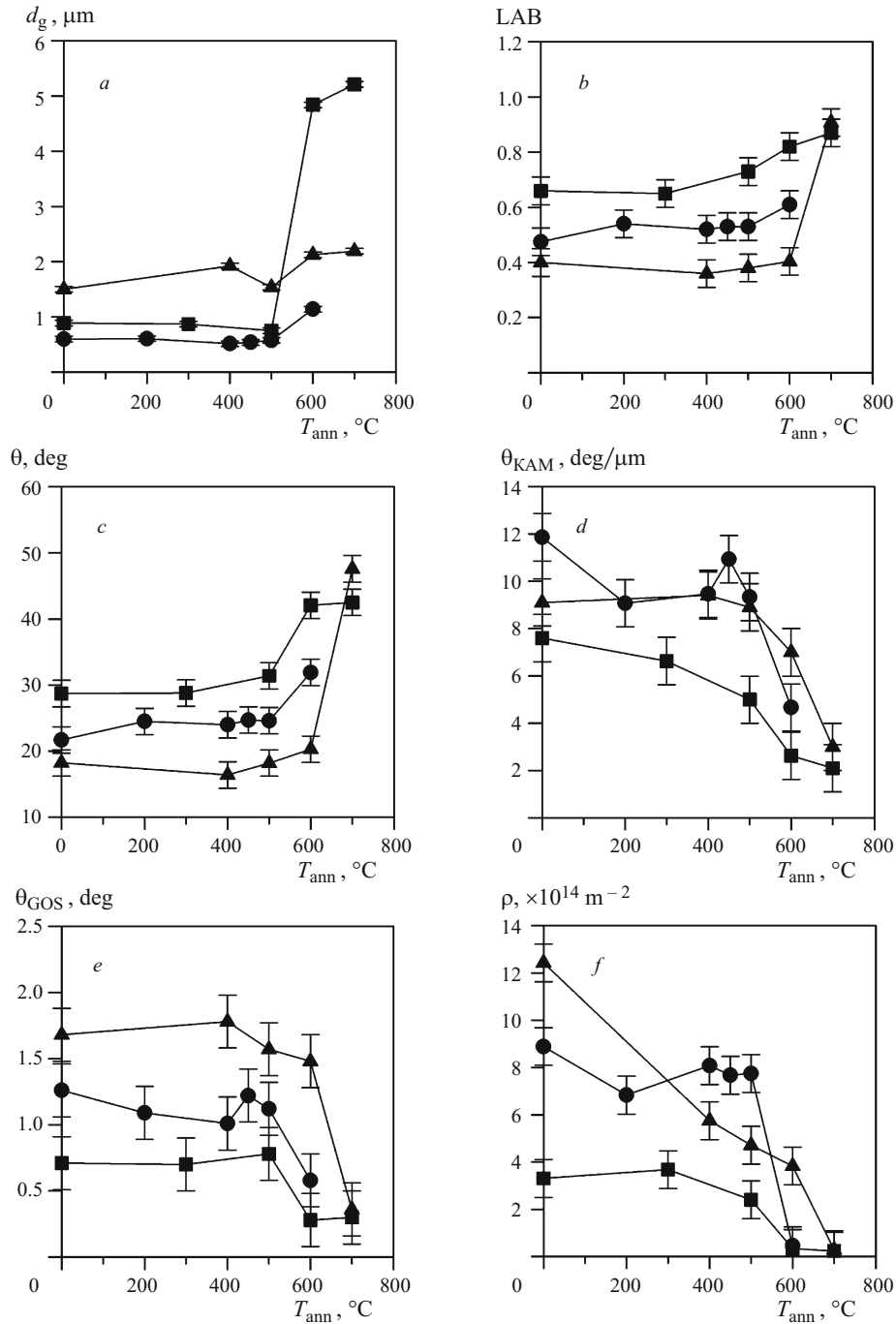


**Fig. 3.** Dependence of grain size  $d_g$  (a), proportion of LAB (b), average crystallite misorientation angle  $\theta$  (c), microdeformation  $\theta_{KAM}$  (d), scatter of misorientations within the limit of a grain  $\theta_{GOS}$  (e), and dislocation density  $\rho$  (f) on alloy annealing temperature ( $T_{ann}$ ): ■ Cu – 0.1Cr – 0.1Zr; ● Cu – 0.9Cr – 0.1Zr; ▲ Cu – 0.3Cr – 0.5Zr.

0.3Cr – 0.5Zr deformed sections are retained. Alongside grains free from internal defects, regions are encountered with a high level of microdeformation and scatter on intragranular misorientations.

Curves are provided in Fig. 3 for the dependence of Cu – Cr – Zr alloy microstructure parameter on annealing temperature. In low-alloy copper alloy Cu – 0.1Cr – 0.1Zr

the average grain diameter (GD) is almost unchanged up to 500 °C and comprises 0.8 – 0.9 μm. However, after annealing at temperatures above 600 °C as a result of development of recrystallization the average grain size increases considerably (up to about 5 μm). Within Cu – 0.9Cr – 0.1Zr and Cu – 0.3Cr – 0.5Zr alloys with an increase alloying element content after annealing at a temperature above 600 °C the aver-

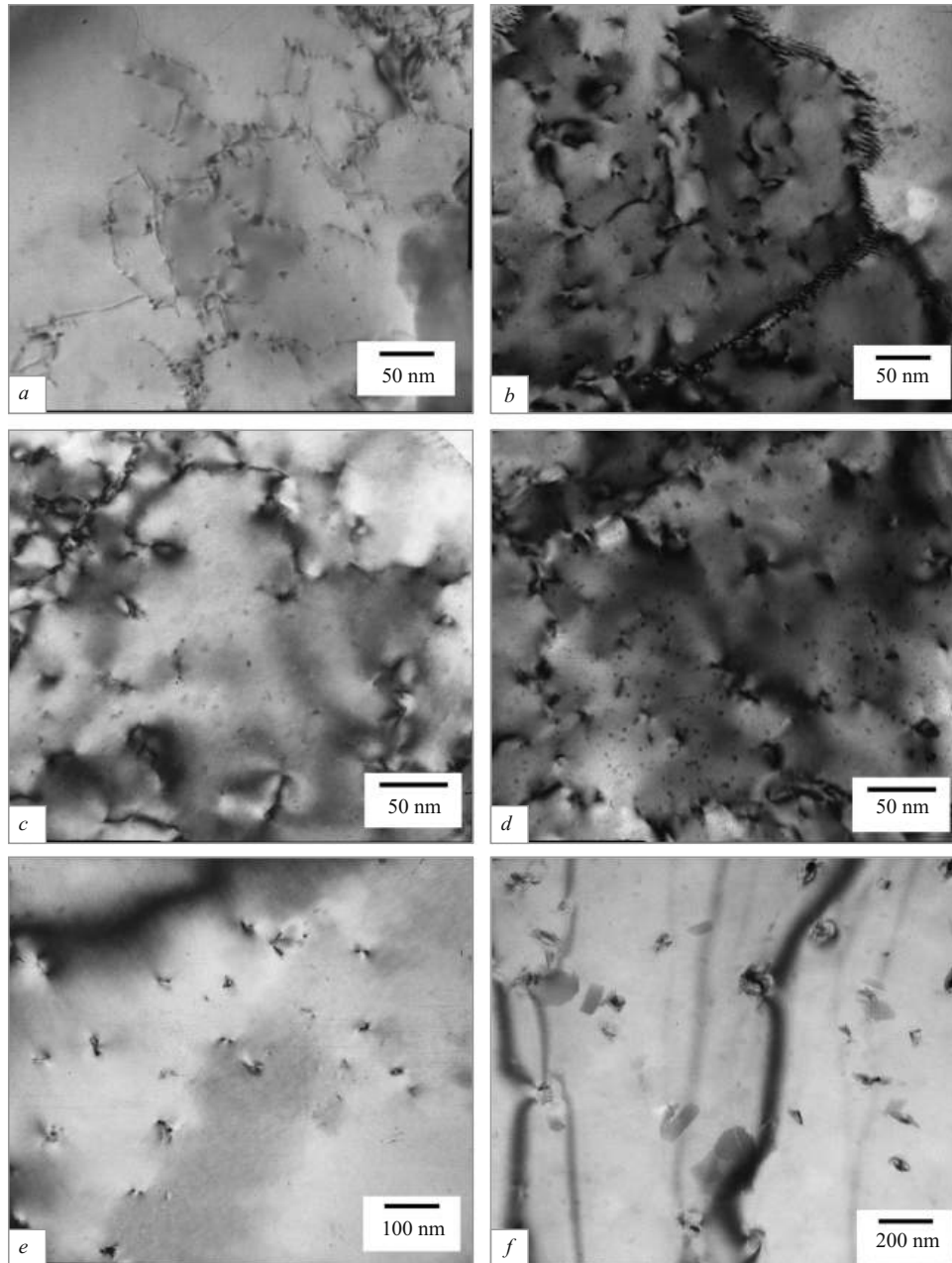


**Fig. 4.** Structure (SEM) of alloys Cu – 0.1Cr – 0.1Zr (*a, c, e*) and Cu – 0.3Cr – 0.5Zr (*b, d, f*): after deformation (*a, b*), deformation and annealing at 500°C (*c, d*) and 600°C (*e, f*).

age grain size does not change so much as within regions with a deformed structure:  $d_g = 1.14$  and  $2.13 \mu\text{m}$  respectively. Development of static recrystallization is accompanied by an increase in the proportion of LAB, and the average boundary misorientation angle. The rate of increase in the proportion of LAB and average misorientation increase after annealing with  $T_{\text{ann}} > 600^\circ\text{C}$ , reaching after annealing at  $700^\circ\text{C}$  values of 0.9 and  $42 - 48^\circ$  respectively, outside the dependence on alloy chemical composition. The average value of microdeformation after ECAP forced within Cu – Cr – Zr-alloys changes in the range  $8 - 12 \text{ deg}/\mu\text{m}$ . Af-

ter annealing at  $200 - 500^\circ\text{C}$  microdeformation within alloy Cu – 0.9Cr – 0.1Zr varies within the range  $9 - 11 \text{ deg}/\mu\text{m}$ . In contrast to this within alloys Cu – 0.1Cr – 0.1Zr and Cu – 0.3Cr – 0.5Zr there is a gradual reduction in microdeformation from  $8$  to  $5 \text{ deg}/\mu\text{m}$ . An increase in annealing temperature from  $600^\circ\text{C}$  to  $700^\circ\text{C}$  leads to a sharp reduction in microdeformation to  $2 - 5 \text{ deg}/\mu\text{m}$  independent of the chemical composition as a result of development of static recrystallization. The average scatter of misorientation within a grain is determined by the chemical composition and annealing temperature. The maximum scatter in misorientation

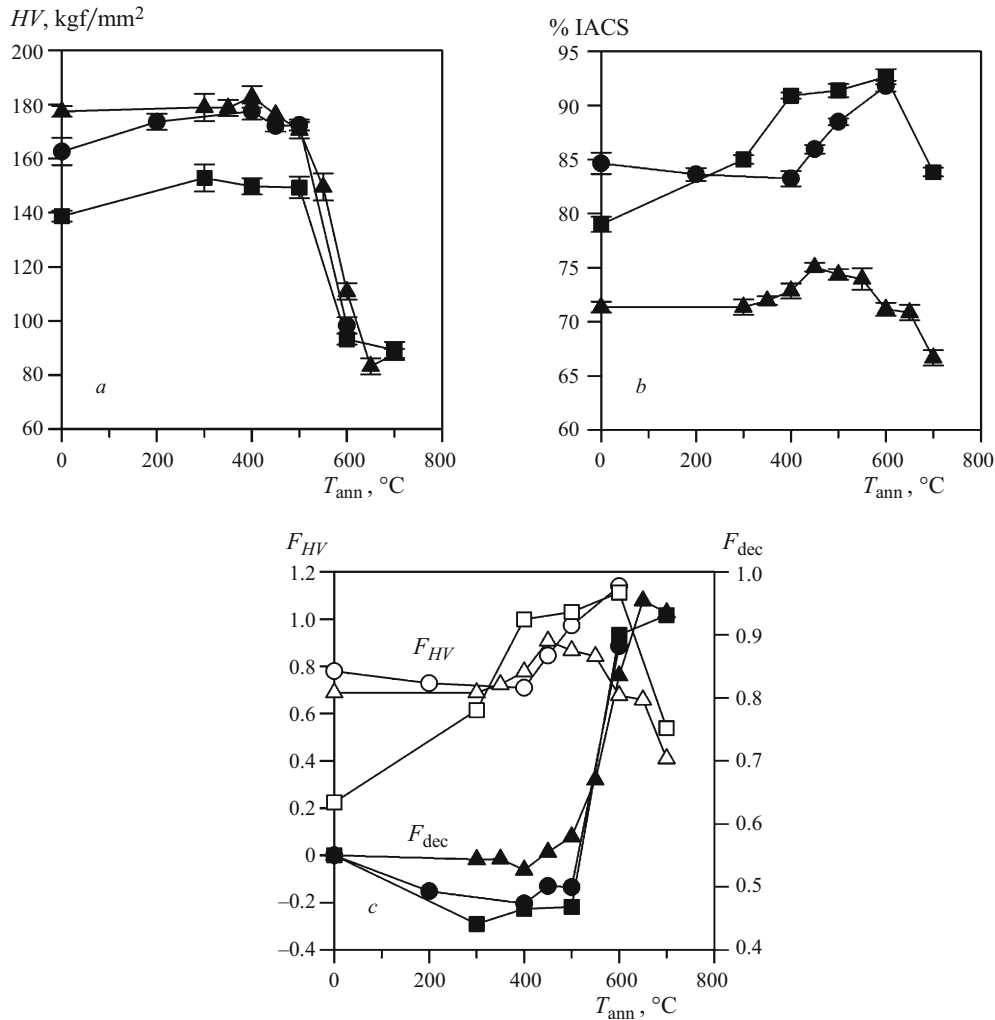


**Fig. 5.** Dependence of hardness ( $HV$ ) (a), electrical conductivity (% IACS) (b), weakening ( $F_{HV}$ ) and proportion of solid solution decomposition ( $F_{dec}$ ) (c) on alloy annealing temperature ( $T_{ann}$ ): ■, □) Cu – 0.1Cr – 0.1Zr; ●, ○) Cu – 0.9Cr – 0.1Zr; ▲, △) Cu – 0.3Cr – 0.5Zr.

within a grain (above  $1.5^\circ$ ) is observed within alloy Cu – 0.3Cr – 0.5Zr after deformation and annealing at 200 – 600°C, and the minimum misorientation (less than  $0.8^\circ$ ) is observed within alloy Cu – 0.1Cr – 0.1Zr after deformation and annealing at 200 – 500°C. After annealing at temperatures above 600°C the scatter of misorientation within a grain decreases considerably. An increase in annealing temperature to 700°C leads to a reduction in scatter of misorientations within a grain to  $0.3 - 0.6^\circ$  independent of the chemical composition. Dislocation density is weakly reduced after annealing at temperatures up to 500°C. An increase in annealing temperature to more than 600°C leads to a reduction in dislocation density within Cu – Cr – Zr alloys by almost an order of magnitude.

After deformation within the structure of low-alloy copper alloys fine particles are observed with sizes of 2 – 5 nm (Fig. 4). Within Cu – 0.1Cr – 0.1Zr the volume fraction of particles is smaller than within alloys with a higher alloying element content. Annealing with  $T_{ann} = 500^\circ\text{C}$  leads to ap-

pearance of fine particles, and their size remains within the range 3 – 5 nm. An increase in annealing temperature to 600°C is accompanied by an increase in fine particles, which acquire a lens shape. The longitudinal size of particles is 10 – 15 nm the transverse size is 3 – 5 nm.

**Hardness and electrical conductivity.** Results of determining hardness and electrical conductivity of alloys of the Cu – Cr – Zr system are provided in Fig. 5. Alloys Cu – 0.9Cr – 0.1Zr and Cu – 0.3Cr – 0.5Zr have similar values of hardness both after deformation (170 – 180  $HV$ ) and after annealing. After annealing at 300 – 400°C an increase in hardness is observed by 5 – 10  $HV$  within all alloys. A significant loss of strength is observed after annealing at 600°C: the hardness of alloys Cu – 0.1Cr – 0.1Zr; Cu – 0.9Cr – 0.1Zr; Cu – 0.3Cr – 0.5Zr comprises 93  $HV$ , 98  $HV$ , and 111  $HV$  respectively. After annealing at 700°C alloy hardness does not depend upon chemical composition and does not exceed 90  $HV$ .

Electrical conductivity increases with an increase in annealing temperature. After deformation of Cu – 0.1Cr – 0.1Zr, Cu – 0.9Cr – 0.1Zr, Cu – 0.3Cr – 0.5Zr alloys their conductivity equals 79% IACS, 85% IACS, 71% IACS respectively. The maximum conductivity within alloys Cu – 0.1Cr – 0.1Zr alloys Cu – 0.9Cr – 0.1Zr is observed after annealing at 600°C and it reaches 92 – 93% IACS. In this case the rate of increase in electrical conductivity is higher within alloy Cu – 0.1Cr – 0.1Zr. After annealing at 400°C the electrical conductivity of Cu – 0.1Cr – 0.1Zr and Cu – 0.9Cr – 0.1Zr alloys comprises 91% IACS and 86% IACS respectively. For alloy Cu – 0.3Cr – 0.5Zr a higher electrical conductivity (75% IACS) is observed after annealing 450°C. A further increase in annealing temperature for this alloy leads to a gradual reduction in conduction properties. i.e., by up to 66% is the IACS after annealing at 700°C. In contrast to this after similar treatment the electrical conductivity of alloy Cu – 0.1Cr – 0.1Zr comprises 84% IACS.

The maximum proportion of supersaturated solid solution within the composition is observed within alloy with the minimum alloying element content (Fig. 5c). Within alloy Cu – 0.1Cr – 0.1Zr during annealing up to 30% of particles may be separated. This facilitates an increase in the amount of obstacles for dislocation movement and fastening, which provides a maximum relative increase in alloys Cu – 0.1Cr – 0.1Zr hardness after annealing compared with the rest of the test alloys.

**Recovery and recrystallization kinetics.** A reduction in dislocation density after annealing is connected with recovery, which includes annihilation of dislocations of different signs, absorption of dislocations by grain boundaries, and coalescence of subgrain boundaries [32, 33]. Knowing the dislocation density within deformed ( $\rho_{\text{def}}$ ) and entirely recrystallized structure ( $\rho_{\text{rec}}$ ), it is possible to consider the proportion of recovery by an equation [34]:

$$F_{\text{reco}} = \frac{\rho_{\text{def}} - \rho_i}{\rho_{\text{def}} - \rho_{\text{rec}}}, \quad (2)$$

where  $\rho_i$  is current dislocation density.

Grain growth with minimum internal distortions, free from dislocations, is connected with development of recrystallization. As a result of this the proportion of recrystallized grains corresponds to the proportion of grains with low scatter of intragranular misorientations ( $< 1^\circ$ ) [35].

Kinetics for development of recovery and recrystallization are provided in Fig. 6. A change in the proportion of recovery or recrystallization ( $F$ ) in relation to annealing time ( $t$ ) obeys a sigmoidal rule that may be described by an Avrami–Kolmogorov equation [33, 35]:

$$F = 1 - \exp\left(-\left(\frac{t}{\tau_0 \exp(Q/RT)}\right)^n\right), \quad (3)$$

where  $T$  is temperature;  $Q$  is process activation energy, in the case of recovery it equalled  $Q = 48$  kJ/mole [36], in the case

of recrystallization  $Q = 175$  kJ/mole [20];  $R$  is universal gas constant and  $n$  and  $\tau_0$  are constants. With transformation of this expression it is possible to obtain a linear dependence of  $\ln(\ln(1/(1-F)))$  on  $\ln t'$ , where  $t' = t \exp(-Q/RT)$  is thermal compensation time. By means of this relationship it is possible to find constants  $n$  and  $\tau_0$ . Constant  $n$  characterizes the process rate and  $\tau_0$  its incubation period.

It is seen from Fig. 6 that the greatest incubation recovery period is observed within alloy Cu – 0.9Cr – 0.1Zr. The recovery rate within alloys with a high alloying element content is quite similar, and constant  $n$  is approximately 0.3. At the same time, the constant  $n$  for alloy Cu – 0.1Cr – 0.1Zr is higher by almost a factor of three ( $n = 1.03$ ), than for alloys with a higher alloying elements content. in [6] it has been demonstrated that particles, precipitated within alloys Cu – 0.1Cr – 0.1Zr, are inclined towards more accelerated growth at 500 – 600°C than within alloy Cu – 0.9Cr – 0.1Zr which may explain the high rate of recovery during annealing, since particle growth is connected with a reduction in their numerical density, i.e., with a reduction in the number of hindrances for dislocation and subgrain boundary movement.

The greatest incubation period for development of recrystallization is observed within alloys with a high alloying element content. after annealing at 600°C the proportion of recrystallized grains comprises 0.2; 0.8; 1.0 within alloys Cu – 0.3Cr – 0.5Zr, Cu – 0.9Cr – 0.1Zr, and Cu – 0.1Cr – 0.1Zr respectively, i.e., the structure is entirely recrystallized only within alloy Cu – 0.1Cr – 0.1Zr. Recrystallization is connected with grain boundary movement. Addition of chromium and zirconium facilitates an increase in volume fraction of separated particles, which causes an increase in of Ziner forces retarding recrystallization and the incubation period for recrystallization development [32, 33, 37, 38]. Alloys Cu – 0.1Cr – 0.1Zr and Cu – 0.9Cr – 0.1Zr have a similar recrystallization development rate, although it is higher within alloy with the minimum alloying element content.

**Mechanical properties.** Provided in Fig. 7 are “stress – relative elongation” curves for copper alloys after deformation and annealing at different temperatures. Since alloy Cu – 0.1Cr – 0.1Zr contains a smaller amount of alloying elements, ad as a consequence a smaller proportion of fine particles, its tensile curve in a deformed condition is characterized by the least flow stress. The strongest alloy is Cu – 0.9Cr – 0.1Zr, which may be connected with the smallest grain size and greatest dislocation density than for the rest of the alloys studied. After deformation all alloys have a small region of equilibrium elongation, comprising 1 – 2%. Independent of chemical composition deformation is rapidly localized within a specimen neck, which may be connected with the slow mobility of dislocations due to their high density. Annealing facilitates an increase in the equilibrium elongation stage and overall ductility.

Within alloy Cu – 0.1Cr – 0.1Zr there is no significant change in flow stress up to 500°C. Yield strength changes within the range  $\sigma_{0.2} = 370 – 375$  MPa, ultimate strength  $\sigma_r =$

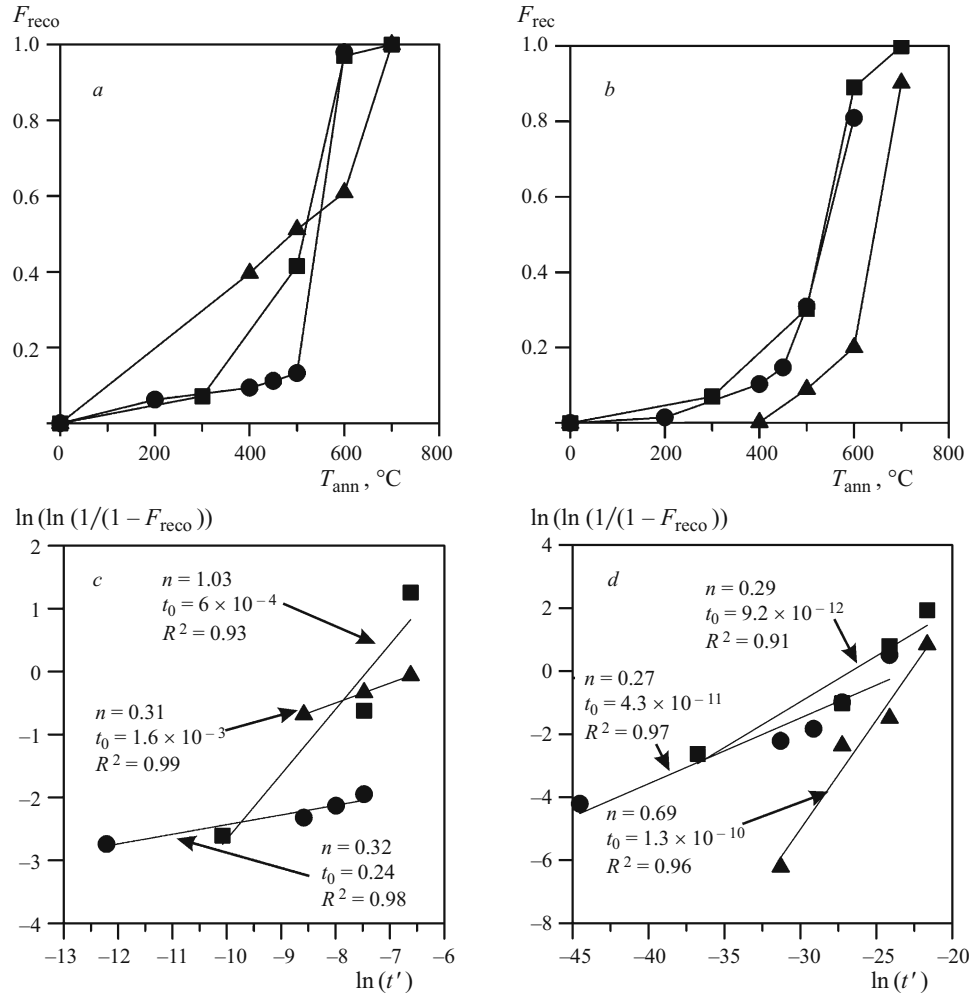


**Fig. 6.** Dependence of proportion of recovery  $F_{\text{reco}}$  (a) and recrystallization  $F_{\text{rec}}$  (b) on alloy annealing temperature ( $T_{\text{ann}}$ ), and also kinetics of these processes on logarithmic coordinates ( $t' = t \exp(-Q/RT)$ ) is temperature-compensation time) (c, d) in alloys: ■ Cu – 0.1Cr – 0.1Zr; ● Cu – 0.9Cr – 0.1Zr; ▲ Cu – 0.3Cr – 0.5Zr.

400 – 405 MPa (Fig. 8). In alloy Cu – 0.9Cr – 0.1Zr strength properties are stable up to 400°C:  $\sigma_{0.2} = 500 – 535$  MPa,  $\sigma_r = 540 – 550$  MPa. Annealing at 500°C causes a reduction in strength properties by 20 MPa.

Annealing alloy Cu – 0.3Cr – 0.5Zr leads to a gradual reduction in strength properties. After annealing at 500°C:  $\sigma_{0.2}$  is reduced from 480 to 380 MPa,  $\sigma_r$  from 510 to 405 MPa. A twofold reduction in strength properties and an increase in ductility properties is observed after annealing at 600 – 700°C within all alloys.

The change in strength properties with an increase in annealing temperature may be connected with several processes: recovery, recrystallization, and separation of fine particles. During recovery there is a reduction in dislocation density and as a consequence a reduction in dislocation strengthening  $\sigma_{\text{disl}}$ , which may be evaluated by means of a Taylor equation:

$$\sigma_{\text{disl}} = \alpha M G b \sqrt{\rho}, \quad (4)$$

where  $\alpha$  is a constant, which normally equals 0.24 [40];  $M$  is Taylor factor, for FCC-materials  $M = 3.06$ ;  $G$  is Young's modulus, for copper  $G = 42.1$  GPa [41],  $b = 2.56 \times 10^{-10}$  m is Burgers factor [42];  $\rho$  is dislocation density.

During recrystallization there is grain growth, free from dislocations. A change in grain boundary strengthening  $\sigma_{\text{H-P}}$  with an increase in annealing temperature may be determined by means of Hall–Petch equation [41];

$$\sigma_{\text{H-P}} = k_y D^{-0.5},$$

where  $k_y$  is Hall-Petch coefficient, for Cu – Cr – Zr alloys  $k_y = 0.11$  [17];  $D$  is grain size.

With an increase in annealing temperature there is an increase in volume fraction and size of fine particles within Cu – Cr – Zr alloys which leads to a change in precipitation hardening. Assuming that within the test alloys dislocation interaction with particles is by an Orowan mechanism, it is

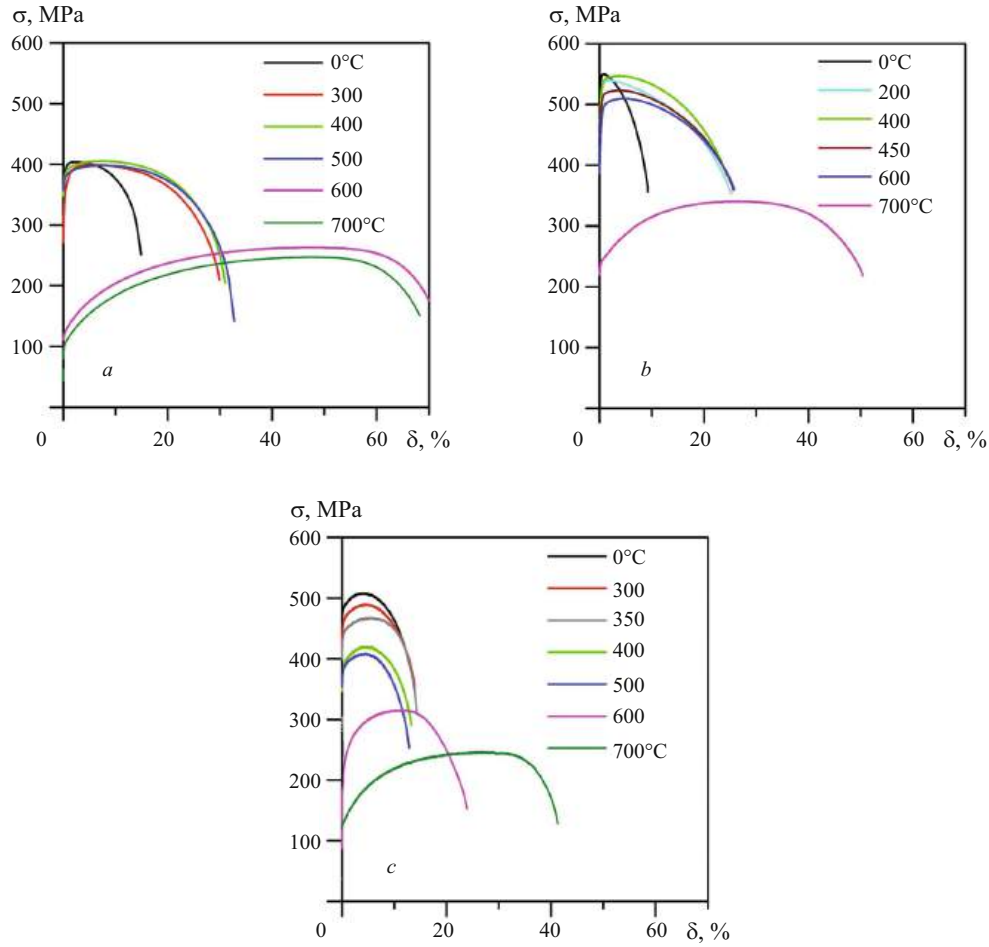


**Fig. 7.** Curves  $\sigma - \delta$ , obtained during tensile tests for alloys Cu – 0.1Cr – 0.1Zr (a), Cu – 0.9Cr – 0.1Zr (b), and Cu – 0.3Cr – 0.5Zr (c) after deformation and annealing at temperatures within the range 0 – 700°C.

possible to calculate the precipitation hardening by the following equation [40]:

$$\sigma_p = \frac{0.4Mgb \ln(2R/b)}{\pi\lambda\sqrt{1-\nu}}, \quad (6)$$

where  $R$  is particle radius;  $\nu = 0.35$  is Poisson coefficient;  $\lambda$  is interparticle distance.

Calculated and experimental results are provided in Table 2 for evaluation of the change in yield strength and the different strengthening contributions for low- and high-alloy materials after annealing at 500 and 600°C compared with a deformed condition. It is seen that calculated data are in good agreement with experimental data. Stability of mechanical properties within alloys Cu – 0.1Cr – 0.1Zr in the temperature range 300 – 500°C is due to compensation for a reduc-

**TABLE 2.** Change in Experimental  $\Delta\sigma_{0.2exp}$  and calculated  $\Delta\sigma_{0.2calc}$  Yield Strength and Strengthening Contributions of Cu – Cr – Zr-Alloys after Annealing Compared with a Deformed Condition

Alloy	$T_{ann}, ^\circ C$	$\Delta\sigma_{0.2exp}, MPa$	$\Delta\sigma_{0.2calc}, MPa$	$\Delta\sigma_{disl}, MPa$	$\Delta\sigma_{H-P}, MPa$	$\Delta\sigma_{part}, MPa$
0.1Cr – 0.1Zr	500	0	20	55	– 10	– 25
	600	250	279	176	67	36
0.3Cr – 0.5Zr	500	100	109	111	10	– 12
	600	275	278	138	14	126

**Notations:**  $\Delta\sigma_{0.2exp}$  is the difference in experimental yield strengths after ECAP and ECAP + annealing;  $\Delta\sigma_{0.2calc}$  is the difference of the sum of strengthening contributions (dislocation, grain boundary, and dispersion) after ECAP and ECAP + annealing;  $\Delta\sigma_{disl}$ ,  $\Delta\sigma_{H-P}$ , and  $\Delta\sigma_{part}$  are the difference in dislocation, grain boundary and dispersion strengthening after ECAP and ECAP + annealing, calculated by Eqs. (4), (5) and (6) respectively.

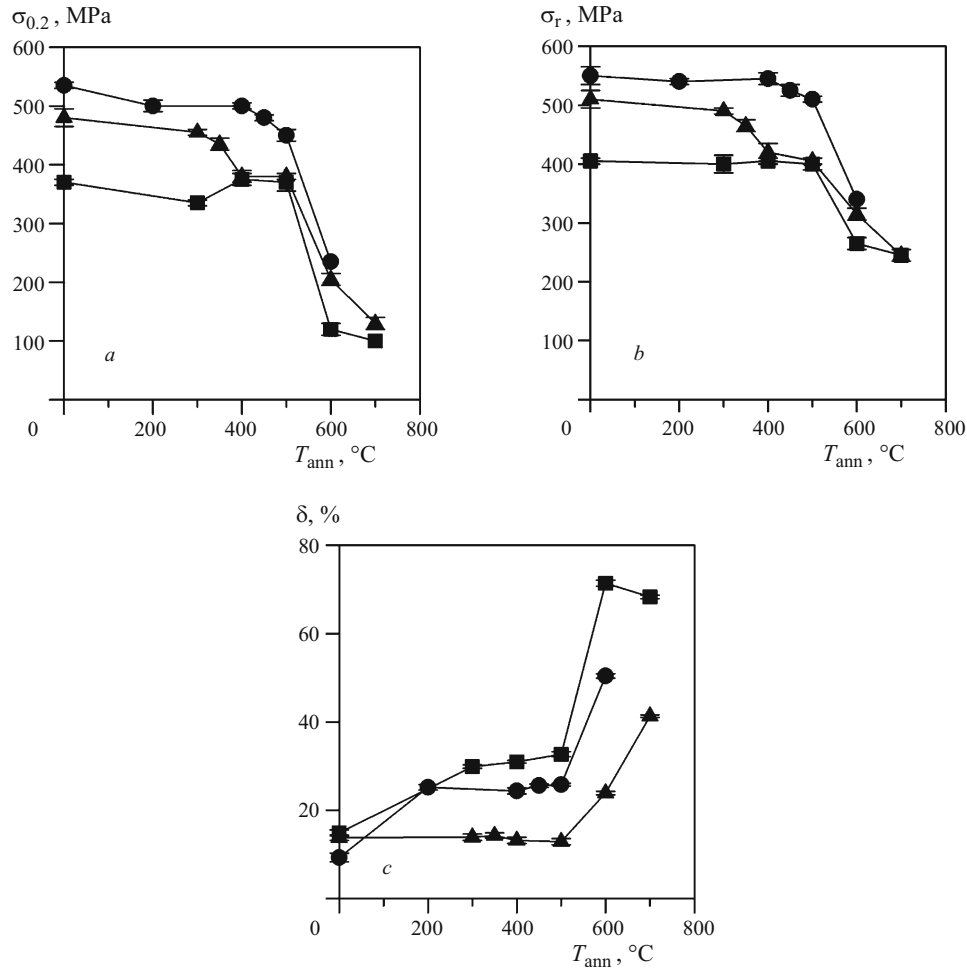


Fig. 8. Dependence of yield strength  $\sigma_{0.2}$  (a), ultimate strength  $\sigma_r$  (b) and relative elongation  $\delta$  (c) on annealing temperature  $T_{ann}$  for alloys: ■) Cu – 0.1Cr – 0.1Zr; ●) Cu – 0.9Cr – 0.1Zr; ▲) Cu – 0.3Cr – 0.5Zr.

tion in strength connected with development of recovery, by an increase in precipitation hardening due to separation of fine particles as a result of breakdown of supersaturated solid solution. At the same time, a significant reduction in dislocation strengthening after annealing at 500°C prevails over precipitation hardening, which leads to a reduction in yield strength by 100 MPa compared with this value for alloy in a deformed condition. Annealing at 600°C leads to particle growth and development of recrystallization, and as a consequence to a significant reduction in all strength factors and overall yield strength to 250 – 275 MPa.

## CONCLUSIONS

Research results for the effect of annealing on evolution of the microstructure, physical and mechanical properties of low-alloy copper alloys of the Cu – Cr – Zr system after deformation make it possible to draw the following conclusions.

1. Annealing at 200 – 500°C leads to development of recovery and reduction in dislocation density within copper al-

loys. An increase in annealing temperature to 600°C facilitates alloy static recrystallization. Within alloy with a low alloying content a fast recovery rate is observed. A high concentration of chromium and zirconium provides an increase in recrystallization incubation period. After annealing alloy Cu – 0.3Cr – 0.5Zr at 600°C the proportion of recrystallized grains within it is 0.2, but within alloy with the minimum chromium content there is formation of a recrystallized structure.

2. Annealing at 200 – 600°C provokes supersaturated solid solution decomposition and delivery of fine particles within alloys. The maximum relative proportion of solid solution breakdown is observed within alloy with the minimum alloying element content.

3. Alloy with a low alloying element content has the least yield strength after deformation, although it has the greatest mechanical property stability after annealing in the temperature range 200 – 500°C. Alloy strength properties with a high chromium and zirconium content in a deformed condition are 100 MPa higher than in alloy with the minimum alloying element content. Annealing at 500°C leads to alloy loss of

strength with a high chromium and zirconium content by 85 – 100 MPa.

4. The stability of alloy properties with a low alloying element content after annealing in the temperature range 200 – 500°C is explained by compensation of the reduction in dislocation strengthening by an increase in precipitation hardening. Within alloys with a high alloying element content a relatively small change in the proportion of supersaturated solid solution decomposition and development of recovery causes a reduction in yield strength. Particle growth and development of recrystallization after annealing at 600°C leads to alloy mechanical property degradation independent of the degree of alloying, although for alloys with a high alloying element content strength properties are 50 – 150 MPa higher than for low-alloy material.

*The investigation was carried out using equipment of the Joint Research Center “Technology and Materials” of Belgorod State National Research University.*

*This work was supported by intra-university “BelSU” grant “Young leaders in science” as part of the project “Science of the 21st century” of the program “Priority-2030.”*

## DECLARATIONS

### Acknowledgments

The investigation was carried out using equipment of the Joint Research Center “Technology and Materials” of Belgorod State National Research University.

### Funding

This work was supported by intra-university “BelSU” grant “Young leaders in science” as part of the project “Science of the 21st century” of the program “Priority-2030”.

### Credit Authorship Contribution Statement

*A. Bodyakova*: conceptualization, methodology, formal analysis, investigation, writing and editing-original draft; *R. Mishnev*: formal analysis, investigation; *R. Kaibyshev*: conceptualization, resources.

### Declaration of Competing Interest

The authors confirm that they have no known financial or interpersonal conflicts that would have appeared to have an impact on the research presented in this study. We are approving the final version of the manuscript.

### Availability of Data and Material

The corresponding author declares on behalf of all authors that all raw data and materials discussed in the study will be freely accessible to any researcher who wants to utilise them for non-commercial research without compromising participant privacy. The corresponding author additionally provides

information on where, if applicable, data might be accessed to support the findings described in the paper.

### Code Availability

Not applicable.

## REFERENCES

1. G. Purcek, H. Yana, M. Demirtas, et al., “Microstructural, mechanical and tribological properties of ultrafine-grained Cu – Cr – Zr alloy processed by high pressure torsion,” *J. Alloys Compd.*, **816**, Art. 152675 (2020).
2. D. A. Aksenov, G. I. Raab, R. N. Asfandiyarov, et al., “Effect of Cd and SPD on structure, physical, mechanical, and operational properties of alloy of Cu – Cr – Zr,” *Rev. Adv. Mater. Sci.*, **59**(1), 506 – 513 (2020).
3. I. S. Batra, G. K. Dey, U. D. Kulkarni, and S. Banerjee, “Microstructure and properties of a Cu – Cr – Zr alloy,” *J. Nucl. Mater.*, **299**(2), 9 – 100 (2001).
4. Yu. R. Nurieva, D. A. Aksenov, R. N. Asfandiyarov, and G. I. Raab, “Mechanical properties and structure of laboratory specimens of contact conductor of Cu – Cr alloy,” *Materials Technologies. Design*, **3**[4(6)], 48 – 53 (2021).
5. V. I. Zel'dovich, S. V. Dobatkin, N. Yu. Frolova, et al., “Mechanical properties and structure of chromium-zirconium bronze after dynamic angular-channel pressing and subsequent aging,” *Fiz. Met. Metalloved.*, **117**(1), 79 (2021).
6. A. Bodyakova, R. Mishnev, A. Belyakov, and R. Kaibyshev, “Effect of chromium content on precipitation in Cu – Cr – Zr alloys,” *J. Mater. Sci.*, **57**(27), 13043 – 13059 (2022).
7. D. V. Shangina, N. R. Bochvar, A. I. Morozova, et al., “Effect of chromium and zirconium content on structure, strength and electrical conductivity of Cu – Cr – Zr alloys after high pressure torsion,” *Mater. Lett.*, **199**, 46 – 49 (2017).
8. R. G. Chembarisova, A. V. Galaktinova, and A. M. Yamilova, “Evolution of secondary phase particles within alloys of the system Cu – Cr – Zr with a limiting low concentration of solid solution in the process of deformation-heat treatment,” *Fiz. Met. Metalloved.*, **122**(1), 45 – 52 (2021).
9. R. K. Islamgaliev, K. M. Nesterov, J. Bourgon, et al., “Nanostructured Cu – Cr alloy with high strength and electrical conductivity,” *J. Appl. Phys.*, **115**, Art. 19 (2014).
10. A. Morozova, R. Mishnev, A. Belyakov, and R. Kaibyshev, “Microstructure and properties of fine grained Cu – Cr – Zr alloys after thermo-mechanical treatments,” *Rev. Adv. Mater. Sci.*, **54**(1), 56 – 92 (2018).
11. M. Y. Murashkin, I. Sabirov, X. Sauvage, and R. Z. Valiev, “Nanostructured Al and Cu alloys with superior strength and electrical conductivity,” *J. Mater. Sci.*, **51**(1), 33 – 49 (2016).
12. R. Z. Valiev, R. K. Islamgaliev, and I. V. Alexandrov, “Bulk nanostructured materials from severe plastic deformation,” *Prog. Mater. Sci.*, **45**(2), 103 – 189 (2000).
13. G. J. Raab, R. Z. Valiev T. C. Lowe, and Y. T. Zhu, “Continuous processing of ultrafine grained Al by ECAP–Conform,” *Mater. Sci. Eng. A*, **382**(1 – 2), 30 – 34 (2004).
14. R. N. Asfandiyarov, G. I. Raab, ad D. A. Aksenov, “Study of the combined severe plastic deformation techniques applied to produce contact wire for high-speed railway lines,” *Metals*, **10**(11), Art. 1476 (2020).
15. A. P. Zhilyaev, I. Shakhova, A. Morozova, et al., “Grain refinement kinetics and strengthening mechanisms in Cu – 0.3Cr –

- 0.5Zr alloy subjected to intense plastic deformation,” *Mater. Sci. Eng. A*, **654**, 131 – 142 (2016).
16. A. Morozova and R. Kaibyshev, “Grain refinement and strengthening of a Cu – 0.1Cr – 0.06Zr alloy subjected to equal channel angular pressing,” *Philos. Mag.*, **97**(24), 2053 – 2076 (2017).
  17. R. Mishnev, I. Shakhova, A. Belyakov, and R. Kaibyshev, “Deformation microstructures, strengthening mechanisms, and electrical conductivity in a Cu – Cr – Zr alloy,” *Mater. Sci. Eng. A*, **629**, 29 – 40 (2015).
  18. W. Q. Cao, C. F. Gu, E. V. Pereloma, and C. H. Davies, “Stored energy, vacancies and thermal stability of ultra-fine grained copper,” *Mater. Sci. Eng. A*, **492**(1 – 2), 74 – 79 (2008).
  19. K. Abib, H. Azzeddine, K. Tirsatine, et al., “Thermal stability of Cu – Cr – Zr alloy processed by equal-channel angular pressing,” *Mater. Charact.*, **118**, 527 – 534 (2016).
  20. Y. D. Wang, F. C. Liu, P. Xue, et al., “Thermal stability behavior of ultrafine-grained Cu – Cr – Zr alloy processed by friction stir processing and rolling methods,” *J. Alloys Compd.*, **950**, Art. 169957 (2023).
  21. Y. Wang, R. Fu, Y. Li, and L. Zhao, “A high strength and high electrical conductivity Cu – Cr – Zr alloy fabricated by cryogenic friction stir processing and subsequent annealing treatment,” *Mater. Sci. Eng. A*, **755**, 166 – 169 (2019).
  22. X. Chen, F. Jiang, J. Jiang, et al., “Precipitation, recrystallization, and evolution of annealing twins in a Cu – Cr – Zr alloy,” *Metals*, **8**(4), Art. 227 (2018).
  23. I. V. Khomskaya, V. I. Zel’dovich, N. Y. Frolova, et al., “Effect of high-speed dynamic channel angular pressing and aging on the microstructure and properties of Cu – Cr – Zr alloys,” *IOP Conf. Ser.: Mater. Sci. Eng.*, **447**(1), Art. 012007 (2018).
  24. V. I. Zel’dovich, I. V. Khomskaya, N. Yu. Frolova, et al., “Structure of chromium-zirconium bronze subjected to dynamic channel-angular pressing and aging,” *Fiz. Met. Metalloved.*, **114**(5), 449 (2013).
  25. V. I. Zel’dovich, N. Yu. Frolova, I. V. Khanskaya, et al., “Structure and microhardness of chromium-zirconium bronze subjected to intense plastic deformation by equal-channel angular pressing and subjected to heating,” *Fiz. Met. Metalloved.*, **115**(5), 495 (2014).
  26. D. V. Pan’gina, N. R. Bochvar, and S. V. Dobatkin, “Structure and properties of Cu – Cr alloys after shear under pressure and subsequent heating,” *Metally*, No. 6, 66 – 72 (2010).
  27. D. V. Pan’gina, Yu. M. Maksimenkova, N. R. Bochvar, and S. V. Dobatkin, “Behavior during heating of ultra fine grained Cu – Zr alloy,” *Metally*, No. 6, 53 (2011).
  28. G. Purcek, Y. Harun, D. V. Shangina, et al., “Influence of high pressure torsion-induced grain refinement and subsequent aging on tribological properties of Cu – Cr – Zr alloy,” *J. Alloys Compd.*, **742**, 325 – 333 (2018).
  29. N. Hansen, “Hall–Petch relation and boundary strengthening,” *Scr. Mater.*, **51**(8), 801 – 806 (2004).
  30. A. V. Nokhrin, N. V. Melekhin, and V. N. Chuvil’deev, “Analysis of the kinetics of supersaturated solid solution decomposition within cast and microcrystalline Cu – Cr – Zr alloy,” *Vestn. Ross. Univ., Matematika*, **16**(3), 821 – 823 (2011).
  31. A. I. Morozova, A. N. Belyakov, and R. O. Kaibyshev, “Effect of deformation temperature on formation of an ultrafine structure within thermally strengthened Cu – Cr – Zr alloy,” *Fiz. Met. Metalloved.*, **122**(1), 67 – 73 (2021).
  32. F. J. Humphreys and M. Hatherly, *Recrystallization and Related Annealing Phenomena*, Elsevier, Amsterdam (2012).
  33. S. S. Gorelik, *Recrystallization of Metals and Alloys* [in Russian], MiSIS, Moscow (2005).
  34. X. Quelenec and J. Jonas, “Simulation of austenite flow curves under industrial rolling conditions using a physical dynamic recrystallization model,” *ISIJ Int.*, **52**(6), 1145 – 1152 (2012).
  35. A. Morozova, O. Dolzhenko, M. Odnobokova, et al., “Annealing behavior and kinetics of primary recrystallization of copper,” *Defect Diffus. Forum*, **385**, 343 – 348 (2018).
  36. C. M. Kuo and C. S. Lin, “Static recovery activation energy of pure copper at room temperature,” *Scr. Mater.*, **57**(8), 667 – 670 (2007).
  37. M. Pa, M. Ferry, and T. Chandra, “Five decades of the Zener equation,” *ISIJ Int.*, **38**(9), 913 – 924 (1998).
  38. A. Morozova, A. Belyakov, and R. Kaibyshev, “Effect of annealing treatment on ECAP structure in Cu – Cr – Zr bronze,” *AIP Conf. Proc.*, **1909**(1), Art. 020142 (2017).
  39. J. W. Taylor, “Dislocation dynamics and dynamic yielding,” *J. Appl. Phys.*, **36**(10), 3146 – 3150 (1965).
  40. T. J. Harrell, T. D. Topping, H. Wen, et al., “Microstructure and strengthening mechanisms in an ultrafine grained Al – Mg – Sc alloy produced by powder metallurgy,” *Metall. Mater. Trans. A*, **45**, 6329 – 6343 (2014).
  41. J. H. Schneibel and M. Heilmaier, “Hall–Petch breakdown at elevated temperatures,” *Mater. Trans.*, **55**(1), 44 – 51 (2014).
  42. K. C. Russell and L. M. Brown, “A dispersion strengthening model based on differing elastic moduli applied to the iron-copper system,” *Acta Metall.*, **20**(7), 969 – 974 (1972).